IETA International Information and Engineering Technology Association

International Journal of Heat and Technology

Vol. 43, No. 1, February, 2025, pp. 1-10

Journal homepage: http://iieta.org/journals/ijht

Numerical Study on Thermal Management of Electric Vehicle Battery Cooling Modules Using Al₂O₃ Nanofluids



Mario Dolmos Chávez[®], Diego Vera Sullayme[®], Yuri Silva Vidal[®], José Villanueva Salazar[®], José Canazas^{*®}, Christofer Diaz[®]

Department of Mechanical Engineering, Universidad Nacional de San Agustín de Arequipa, Arequipa 04000, Peru

Corresponding Author Email: jcanazas@unsa.edu.pe

Copyright: ©2025 The authors. This article is published by IIETA and is licensed under the CC BY 4.0 license (http://creativecommons.org/licenses/by/4.0/).

https://doi.org/10.18280/ijht.430101

Received: 1 December 2024 Revised: 4 February 2025 Accepted: 16 February 2025 Available online: 28 February 2025

11,414,210 0111110 2010

Keywords:

nanofluids, electric vehicles, battery, cooling system, serpentine tube

ABSTRACT

The battery cooling system of electric vehicles (EV) is one of its most important systems. A proper cooling system has a major effect on energy storage, durability, life cycle and efficiency. As a result, the selection of an effective cooling mechanism for an EV battery module is critical to maintain the temperature within the proper range. A numerical study of a serpentine tube used in EV battery cooling system is carried out. Two arrangements of the serpentine tube are proposed in addition to the conventional one to evaluate its performance. Aluminum oxide nanoparticles suspended in water and ethylene glycol as coolant were investigated at volume concentrations of 0.5%, 1.0% and 1.5%. The results indicated that the serpentine tube arrangements improved the temperature distribution and reduced the pressure drop. The incorporation of nanoparticles also decreased the maximum temperature of the system by modifying the thermophysical properties, although this caused an increase in pressure drop due to the higher viscosity of the fluid. It is concluded that the arrangement of the serpentine tube and the use of nanofluids influences the thermal and hydraulic performance and presents an alternative to optimize this type of thermal systems.

1. INTRODUCTION

The energy problem of our times and the environmental pollution caused by the automotive sector is a problem to be solved [1]. In response, electric vehicles (EVs) have become more popular due to their cleaner and more environmentally friendly operation by switching from the use of fossil fuels to electric power from renewable sources [2]. However, despite their great benefits, EVs face challenges such as battery overheating in full operation, especially when operating under intense charging and discharging conditions. These batteries, which are mostly lithium-ion, tend to generate high temperatures, which exposes them to a reduction in their useful life, performance and endangers the safety of operators [3]. It is therefore vitally important to develop and optimize both the structural and energy aspects of these cooling systems.

The technology of these cooling systems consists of a wavy serpentine tube covered with thermally conductive and electrically insulating material that moderates the temperature inside the module while also insulating the cells from each other [4, 5]. However, at the structural level, the implementation of new materials or the use of finned or louvered surfaces can promote improvements in heat transfer [6].

Likewise, the use of water and ethylene glycol solutions as a working fluid is widely used in EV cooling systems [7, 8]. In this area, the use of nanofluids, nanoscale colloidal solutions consisting of nanoparticles (with sizes on the order of 1 to 100 nm) dispersed in a base fluid, have been of interest to researchers in recent decades. When nanoparticles are uniformly dispersed in base fluids, the resulting suspension shows a remarkable improvement in its thermal properties [9]. Several works in the literature have applied nanofluids in thermosyphons, electronic cooling modules, heat pipes, microchannel heat sinks, heat exchangers, refrigeration systems, among others [10]. Therefore, its application in EV cooling systems can promote improved heat transfer and ensure optimal battery operation and performance.

Among the various studies on analysis and improvements in EV battery cooling systems, Singh et al. [11] studied forced air convection cooling of lithium-ion batteries. According to their results, the distribution of the batteries did not have a significant influence on the maximum temperature of the system. Zhao et al. [12] also did a review of cooling systems using air, which despite not being as efficient as other methods, in their work they improved the design of the cooling channels with fins and flaps in the inlet, outlet and secondary channel to improve convective heat transfer. Xiao et al. [13] developed a cooling system composed of a Phase Change Material together with liquid cooling, where it was seen that by increasing the space between the batteries and increasing the flow, overheating is delayed. Zhang and Wei [14] reported a system using flat heat pipes for prismatic type battery packs, compared with other two systems which are natural air convection and aluminum plate cooling, the use of flat heat pipes improved the heat dissipation and made the temperature

more uniform. Xu et al. [15] studied a method based on minichannel cooling, in this system thermal decontrol occurs in a single individual cell, but when tested throughout the entire module, the opposite happens. Aldosry et al. [16] highlighted the importance of using finned surfaces in cooling efficiency in EV battery thermal management, here ethylene glycol and water are used in different proportions to see which is the most appropriate. It was observed that the ratio 75% water and 25% ethylene glycol was the most optimal. Chung and Kim [17] presented a design with finned surfaces and said that the asymmetric design of the fins is detrimental to the temperature uniformity, in this case the batteries are pouch type, this new design benefits the temperature uniformity by reducing weight, pressure drop and volume. Saw et al. [18] also propose the fins with pouch type battery but these batteries are lithium ferrophosphate using aluminum foam in different porosities and pore densities to see which combination is better, this foam forms a cooling plate that helps to control the temperature, having as a result that 10 PPI with porosity of 0.918 in the foam has a better thermal performance. In the work of Pety et al. [19] a novel battery packaging is presented using carbon/epoxy microvascular panels with 2D channel networks that will serve to protect the batteries from impacts and maintain the temperature at a suitable value. Al-Zareer et al. [20] unveiled a system that uses the liquid to vapor phase change of the fuel inside tubes in an aluminum block surrounding the batteries, where the aluminum transfers heat from the batteries to the coolant in the tubes, this helps improve temperature uniformity and the batteries do not have direct contact with the coolant. A number of review articles provide the benefits and drawbacks of different EV cooling methods, all of which highlight the importance of choosing an effective cooling system to improve the efficiency, safety and useful life of lithium-ion batteries [21-23]. At the individual cell and battery module level, other authors conducted experimental and numerical studies to optimize cooling systems by analyzing heat dissipation in the battery [24]. Jarrett and Kim [25, 26] revealed that the design of the cooling plates, heat flow and coolant volumetric flow play an important role when it comes to see the temperature uniformity in the batteries, they also say that the wider the channels, decreases the pressure drop, so it presents a design where the channel is narrower at the entrance and gradually becomes wider to the exit, to match effects of heat transfer area, coolant velocity and temperature gradient to improve temperature uniformity throughout the system. Kshetrimayum et al. [27] studied the cooling system of 18650 type batteries, where through the application of a phase change material together with a microchannel plate, they observed that the temperature distribution was better and under the desired working conditions. Benabdelaziz et al. [28] proposed four designs of battery cooling plates where they identify that the contact surface between the channels and the battery is of vital importance for proper cooling.

There are many studies in the literature on cooling systems in electric vehicles, which use different methods with the aim of optimizing and improving this process. Among these methods, the application of nanofluids as a working fluid has been of great interest. For example, Ouyang et al. [29] studied the performance of the cooling system using silver oxide nanoparticles in water, considering different volume fractions of the nanoparticles and different flow rates as variables. According to the results, the higher the flow rate, the maximum temperature decreases but the pump power

increases, something similar happens with the percentage of volume fraction of nanoparticles, where the higher the percentage, the lower the system temperature. Sirikasemsuk et al. [30] used in their research a thermoelectric module with pulsed water flow and nanofluids for EV battery cooling where important parameters such as temperatures, heat transfer coefficients, pressure and COP were obtained. Zhou et al. [31] performed an experimental study of a hybrid system of oscillating heat pipes (OHP) with carbon nanotubes based nanofluids in a water-ethanol mixture. This study was done on a hybrid OHP and it is seen that using these nanofluids decreases the average temperature of the system. Sarchami et al. [32] carried out an experimental investigation using silver oxide nanofluids. 21700 batteries were used in this study, specifically for the charging and discharging conditions. The results show that using this nanofluid with 0.28 m/s inlet velocity and 4% volume fraction of the nanoparticle, the 5C charging/discharging processes of the battery pack makes the maximum temperature and temperature diversity stay below 31.55°C and 2.95°C, respectively.

In this work, a numerical study is conducted on the thermal and hydraulic performance of a serpentine tube used in the cooling system of electric vehicle batteries by using three different volume concentrations of aluminum oxide nanoparticles suspended in the working fluid. Also, two novel arrays of the serpentine tube passages in the battery will be proposed, with the objective of identifying an optimal arrangement that guarantees an adequate temperature distribution. On the other hand, also evaluate the pressure drop in the arrangements to be studied, which is directly related to the pumping power in the system. In summary, a study of EV battery cooling is carried out, looking at the impact of using nanofluids as the cooling fluid in this system. As far as we know, previous research has not studied this type of nanofluid for this type of application, and the use of aluminum oxide nanoparticles has some advantages, such as commercial availability, as well as its great interest in thermal systems due to its good performance [33, 34]. The following is, in chapter 2, the methodology used for the work is described, divided into: the description of the system, the mathematical model and the details of the numerical simulation. Then, in chapter 3 the results are presented and it will be discussed which arrangement had an adequate performance, as well as the influence of the use of nanofluids in this type of systems. Finally, in chapter 4 the conclusions as well as future studies of the research work are discussed.

2. METHODOLOGY

In the present work, 18650 cylindrical batteries are used. Battery characteristics such as thermal load, dimensions and number of cylindrical batteries in the array are detailed. This information will be used in computer-aided design and numerical study. Also, it is worth it to mention that these batteries are one of the most widely used in the EV sector, and use the "Side - Cooling Arrangement" cooling technology. This technology has a serpentine tube cooling system producing thermal exchange between the coolant and the tube walls, also being a uniform design that covers all parts that need cooling, avoiding hot spots and improving temperature uniformity. Figure 1 shows three distributions of the tubes passing through the coil arrangement. The first arrangement (Figure 1(a)) is the one conventionally used in EV vehicles.

The other two distributions were proposed with the objective of identifying a better temperature distribution or obtaining a lower pressure drop. In the case of the second arrangement (Figure 1(b)) it was thought that with the multiple changes of direction there will be greater turbulence and therefore greater heat transfer, in addition to the cold fluid at the beginning of the serpentine tube is near the end of the tube, so it can help to cool this area. For the third arrangement (Figure 1(c)), we have in mind that it has fewer changes of direction than the previous geometry and the pump has less energy consumption since the resistance to flow is lower, also that it has a more uniform flow as the first geometry but unlike this, the third geometry recirculates its cold fluid from the beginning by many parts where the fluid at the end is already hot and will help to improve the temperature in greater proportion than in the second geometry.

2.1 System description

2.1.1 Battery 18650

As mentioned above, 18650 batteries are used in this study. Table 1 describes the specifications of this type of batteries. They are distributed along the serpentine tube, in total there are 444 cylindrical batteries. This type of batteries has a great interest in the EV vehicle market with respect to the others due to its options and varieties of purchase, also these batteries are more economical because of its long time in the international market. In addition, they are well accepted for their great performance and reliability. These batteries are small, so you can opt for various configurations and arrangements of cooling systems, complex and customized geometries that optimize the space inside the EV and can improve aspects such as the average working temperature and pressure differential.

2.1.2 Serpentine tube

Serpentine tube cooling has gained a lot of interest in the EV sector compared to other technologies because this geometry brings all the batteries in contact with the coolant. It also helps the batteries to receive a more homogeneous cooling process and to avoid temperature peaks or high temperature differentials as much as possible. Also, this design is relatively simple for the modeling and mass manufacturing process. Additionally, this system has very few moving components and few necessary connections, so it can be easily maintained. Furthermore, this geometry makes it possible to make maximum use of the EV space, since it has a compact design, which is a great advantage since space is a limited resource in

an EV. The specifications of the serpentine tube structure are detailed in Table 2.

Table 1. Battery specifications

Description	Value
Battery type	18650
Battery geometry	Cylindrical
Diameter	18 mm
Height	65 mm
Material	Lithium Ions

Table 2. Serpentine tube specifications

Description	Value
Number of batteries	444
Material	Aluminum
Height	63 mm
Wide	4 mm
Wall thickness	0.5 mm
Working fluid	Water (50%) +
working muid	Ethylene Glycol

2.2 Governing equations and thermophysical correlations

The basic equations for conservation of mass, linear momentum and energy without considering viscous dissipation, buoyancy and energy sources are presented below:

$$\frac{\partial u}{\partial x} + \frac{\partial v}{\partial y} + \frac{\partial w}{\partial z} = 0 \tag{1}$$

$$\rho \left(u \frac{\partial u}{\partial x} + v \frac{\partial u}{\partial y} + w \frac{\partial u}{\partial z} \right) = -\frac{\partial p}{\partial x} + \mu \left(\frac{\partial^2 u}{\partial x^2} + \frac{\partial^2 u}{\partial y^2} + \frac{\partial^2 u}{\partial z^2} \right)$$
(2)

$$\rho \left(u \frac{\partial v}{\partial x} + v \frac{\partial v}{\partial y} + w \frac{\partial v}{\partial z} \right) = -\frac{\partial p}{\partial y} + \mu \left(\frac{\partial^2 v}{\partial x^2} + \frac{\partial^2 v}{\partial y^2} + \frac{\partial^2 v}{\partial z^2} \right)$$
(3)

$$\rho \left(u \frac{\partial w}{\partial x} + v \frac{\partial w}{\partial y} + w \frac{\partial w}{\partial z} \right) = -\frac{\partial p}{\partial z} + \mu \left(\frac{\partial^2 w}{\partial x^2} + \frac{\partial^2 w}{\partial y^2} + \frac{\partial^2 w}{\partial z^2} \right)$$
(4)

$$\rho c \left(u \frac{\partial T}{\partial x} + v \frac{\partial T}{\partial y} + w \frac{\partial T}{\partial z} \right) = k \left(\frac{\partial^2 T}{\partial x^2} + \frac{\partial^2 T}{\partial y^2} + \frac{\partial^2 T}{\partial z^2} \right)$$
 (5)

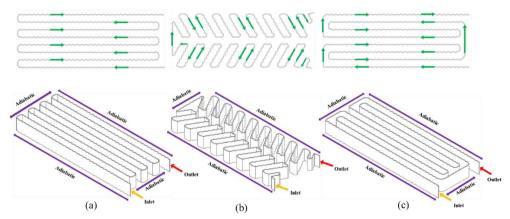


Figure 1. Distribution of the serpentine tube in the battery arrangement. In the upper part is shown the plan view with the flow direction. In the bottom part is shown the isometric view with boundary conditions: (a) Geometry 1, (b) Geometry 2, (c) Geometry 3

Table 3. Correlation of properties EG/W 50:50 para 20°C≤T≤100°C

Property	Correlation	\mathbb{R}^2	Equation
Density (kg/m ³)	$\rho = -0.0024T^2 + 0.9881T + 992.4087$	0.997	(6)
Viscosity (Pa.s)	$\mu = 0.000000549T^2 - 0.0004T + 0.0745$	0.993	(7)
Specific heat (J/kg-K)	$c = 0.0002T^2 + 3.7204T + 2172.6458$	0.999	(8)
Thermal conductivity (W/m-°C)	$k = -0.0000034675T^2 + 0.0027T - 0.1245$	0.999	(9)

These equations are described based on the Cartesian coordinate system and considering 3D Newtonian laminar flow. For the study properties of density, specific heat, dynamic viscosity and thermal conductivity of the base coolant fluid and nanofluids are required, which will be temperature dependent. The data of the base fluid properties were obtained from the ASHRAE Fundamentals Manual [35] and were fitted to a curve as a function of temperature, in a range of $20^{\circ}\text{C} \leq T \leq 100^{\circ}\text{C}$. The thermophysical correlations of the base coolant fluid presented in Table 3 show a coefficient of determination of $R^2 \approx 1$.

The following correlations have been used to predict nanofluid density and specific heat, respectively, at different temperatures and concentrations [34, 36].

$$\rho_{nf} = \phi \rho_p + (1 - \phi) \rho_{bf} \tag{10}$$

$$(\rho c)_{nf} = \phi(\rho c)_{p} + (1 - \phi)(\rho c)_{bf}$$
 (11)

Chiam et al. [37] developed correlations for thermal conductivity and viscosity of ethylene glycol and water with Al_2O_3 nanoparticles.

$$\frac{k_{nf}}{k_{bf}} = 0.9683(1+\phi)^{11.13} \left(1 + \frac{T}{70}\right)^{0.1676} (0.01 + BR)^{0.00111}$$
 (12)

$$\frac{\mu_{nf}}{\mu_{bf}} = (1 + \phi)^{32} \left(\frac{T}{70}\right)^{-0.001} (0.1 + BR)^{0.08}$$
 (13)

From the previous four equations ϕ is the volume fraction of nanoparticles, and BR is the ratio of water to ethylene glycol which in this case is 0.5. In the present study, three different volume concentrations (0.5%, 1.0% and 1.5%) of aluminum oxide nanoparticles suspended in the base working fluid were considered. Also, the density and specific heat of the nanoparticles was considered according to previous studies as 4,000 kg/m³ [37] and 880 J/kg-K [38], respectively.

2.3 Numerical simulation

For the numerical study of the serpentine tube, to solve the equations governing the problem and to implement the thermophysical correlations, Ansys Fluent software is used. First, the proposed serpentine tube arrangements are meshed, as shown in Figure 2. In the analysis process, four grid structure independence tests of the model have been performed. The number of elements is increased in order to identify a value where the temperature has stability in its results. Table 4 shows the different grid elements for each geometry, where it is highlighted for the three geometries consecutively, and the maximum temperatures using the different grids for the base working fluid. In the three geometries, the maximum coolant temperature obtained from

500,000 is finer than those of fewer elements. Therefore, the element numbers of 565,000, 551,099 and 554,962 were chosen for the simulation to ensure a satisfactory solution for geometry 1, geometry 2 and geometry 3, respectively.

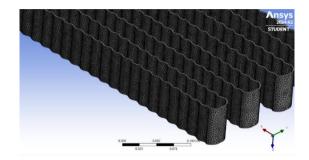


Figure 2. Unstructured tetrahedral mesh system in geometry 1 with 565,000 elements

Table 4. Evaluation of the mesh independence of the 3 geometry models, using the base working fluid

Geometry	Elements	Maximum Temperature (K)	% Difference
Geometry 1	261,399	329.47	-
	400,986	329.50	0.05%
	565,000	330.18	1.20%
	718,393	330.23	0.09%
Geometry 2	250,260	330.62	-
	402,118	332.02	2.44%
	551,099	332.03	0.01%
	701,720	332.05	0.04%
Geometry 3	249,829	330.59	-
	400,076	330.65	0.11%
	554,962	330.74	0.15%
	705,493	330.79	0.08%

Table 5. Properties of the boundary conditions of the refrigeration system

Description	Value	
Inlat	Velocity: 0.09 m/s	
Inlet	Temperature: 293 K	
Outlet	Outflow	
Heat flux from	3,000 W/m ² (Only in the parts where there	
batteries	are batteries)	
	Adiabatic, because there are no batteries in	
Wall	these parts and therefore there will be no heat	
	flow.	

The boundary conditions applied in the numerical analysis are performed under a constant heat flux on the walls where the heat generated by the lithium-ion cylindrical batteries type 18650 has an estimated total of 3,000 W/m² [39]. In this study, the second-order upwind scheme and SIMPLE algorithm are used to solve the numerical problem. The numerical computation ends if the residual summed over all

computational nodes satisfies the 10-4 criterion. Details of the simulation input data are given in Table 5.

3. RESULTS AND DISCUSSIONS

According to the literature review, most of the previous studies were performed by numerical analysis. As a result, this section has no experimental results to support the projected results. However, to obtain the best accurate computational results with the fewest number of elements, four independent tests of the mesh of each proposed geometry were considered, as indicated above. Additionally, the heat flow conditions indicated in this work are maximum working conditions of the battery [39]. This means that the heat generated by the battery cell in real conditions is lower than the condition of this study, but the vehicle is exposed to various unpredictable scenarios that increase the temperature of the batteries to the maximum at certain times and it is difficult to predict these temperature peaks [40], so this maximum heat flux value is used.

Figure 3 shows the temperature variation along the serpentine tube for the three proposed geometries, and using the base working fluid, and the maximum concentration in volume of nanoparticles. First, just analyzing the thermal performance of the base fluid, for geometry 1, it can be observed that using only the base fluid as coolant, a maximum system temperature of 330.18 K is obtained. As the coolant circulates through the serpentine tube, it absorbs the heat generated, then as the coolant circulates, the cooling capacity is reduced, resulting in a moderately homogeneous cooling, with less hot batteries at the inlet. On the other hand, in geometry 2, which was proposed to improve the temperature distribution in relation to the first geometry, it can be identified that the coolant passing through the initial section of the

serpentine tube, also helps to cool to some extent the final section of the system. However, as shown in the results the maximum temperature rose to 332.03 K, probably due to the different contact that the serpentine tube has with the batteries throughout the array. So, even though the temperature distribution had some improvement, it still presents that high temperature concentration in some regions of the system. Finally, for geometry 3, which was made with the objective of having at least one recirculation in the final section of the system to ensure good thermal management. It can be observed in the simulation results that the maximum temperature rose slightly with respect to geometry 1 up to 330.74 K. However, the temperature distribution is much better, since a warm flow of coolant will go to cool the last section of the system, and will not jeopardize the performance and safety of the batteries.

Also Figure 3 shows the influence on the temperature distribution of the maximum concentration of aluminum oxide nanoparticles considered in this study suspended in the working fluid. In all three geometries it can be seen that the addition of nanoparticles resulted in a reduction of the maximum temperature of the system, this decrease is mainly due to the increase of the thermal conductivity in nanofluids [37], therefore, the heat transfer was improved, dissipating more quickly the heat delivered by the batteries. Additionally, it is important to note other properties of interest in heat transfer such as specific heat and density, since together with thermal conductivity they result in thermal diffusivity. This last parameter is also of interest, since during the cooling process in the system it is important to identify how fast our fluid will heat up, which in this case is more dependent on the specific heat. In summary, it is evident to observe the clear decrease in temperature obtained thanks to the good performance of the nanoparticles.

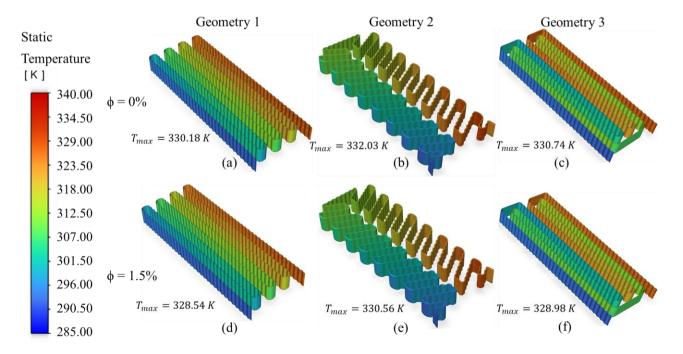


Figure 3. Temperature distribution along the serpentine tube: (a) Geometry 1 - water (50%) and ethylene glycol (50%) as coolant, (b) Geometry 2 - water (50%) and ethylene glycol (50%) as coolant, (c) Geometry 3 - water (50%) and ethylene glycol (50%) as coolant, (d) Geometry 1 - Al₂O₃ nanofluid at 1.5% nanoparticle concentration as coolant, (e) Geometry 2 - Al₂O₃ nanofluid at 1.5% nanoparticle concentration as coolant, (f) Geometry 3 - Al₂O₃ nanofluid at 1.5% nanoparticle concentration as coolant

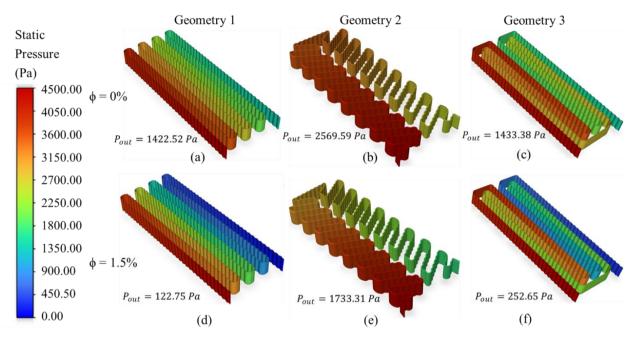


Figure 4. Static pressure distribution along the serpentine tube: (a) geometry 1 - water (50%) and ethylene glycol (50%) as coolant, (b) geometry 2 - water (50%) and ethylene glycol (50%) as coolant, (c) geometry 3 - water (50%) and ethylene glycol (50%) as coolant, (d) geometry 1 - Al₂O₃ nanofluid at 1.5% nanoparticle percentage as coolant, (e) geometry 2 - Al₂O₃ nanofluid at 1.5% nanoparticle percentage as coolant

Figure 4 shows the static pressure distribution. In these closed cooling systems, a pumping system with recirculation is used to ensure continuous operation and tightness. An inlet pressure of 4,500 Pa was considered as an arbitrary value in order to compare the static pressure values in the different geometries and fluids used. The pressure drop obtained in each configuration, which is directly proportional to the pumping power, will be specifically discussed later. It can be observed that for the base fluid, geometry 1 and 3 had a quite similar behavior identified by similar outlet pressures. However, in geometry 2, the outlet pressure was higher, indicating a lower friction loss in the serpentine tube, this was probably due to the fact that in this geometry, in spite of having many curves which causes a higher pressure loss, the total extension of the tube is smaller compared to the other geometries. The addition of nanoparticles, on the other hand, caused a decrease in the outlet pressure of the serpentine tube. This is expected because there is an increase in the viscosity of the nanofluids, which causes greater resistance of the fluid to pass through the tube.

Currently, some other configurations of the serpentine tube arrangement have been proposed, passing through the set of batteries [39]. Although the use of technologies such as the implementation of counter-flow steps in the system can be beneficial from the thermal point of view, the manufacture and maintenance of this type of cooling systems can be more expensive and take more time. In our case, the flow was maintained with a single step, and different results were obtained in heat transfer and pressure drop for each configuration studied. Then, geometry 3 presented a more adequate temperature distribution, and geometry 2 presented a lower pressure drop.

The effect of the different percentages of nanoparticles on the maximum temperature of the system for the 3 geometries is represented in Figure 5, where it can be observed that the higher the percentage of nanoparticles, the maximum temperature decreases, it is observed that geometry 1 presents results with lower maximum temperatures with respect to the others. Although it is appropriate to have lower temperatures, and this was provided by the nanoparticles, it is also important to have a good temperature distribution as discussed above. It can be observed that geometry 1 has as maximum temperature with the base fluid as coolant 330.18 K, improving this temperature by 1.75%, 2.17% and 2.87% for the Al₂O₃ nanofluid with 0.5%, 1.0% and 1.5% concentration in volume of nanoparticles respectively, where it can be seen that 328.54 K is the lowest temperature obtained in the simulation at the concentration of 1.5% of nanoparticles. Keeping this concentration, it can be observed that the maximum temperature is obtained in geometry 2 (330.56 K), from this value geometry 1 presents a percentage improvement of 3.51% in temperature and geometry 3 presents a 2.75% improvement. It can also be perceived that working with nanofluids in cooling systems is better than water - ethylene glycol only, because nanofluids have a higher thermal conductivity, which generates an adequate dissipation of the heat generated by the batteries, maintaining an operating temperature under the critical working levels.

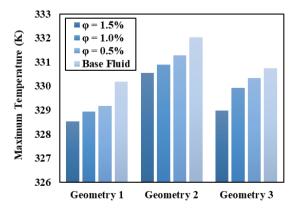


Figure 5. Maximum temperature of the different geometries along the serpentine tube using water - ethylene glycol at 50% each and nanofluids (1.5%, 1.0%, 0.5% nanoparticles) as coolant

Figure 6 shows the pressure drop in the three proposed geometries for the three concentrations of nanoparticles used and the base fluid. As the concentration of nanoparticles increases the pressure drop increases, considering that the volumetric flow of fluid is constant in all cases, the pumping power increases linearly to the pressure drop. If the pumping power is not adequate, the circulation of the cooling fluid may be affected and overheat the batteries. Then, it would be ideal to have a pumping system that works according to the need of the system, and that can be driven in order to maintain an adequate temperature of the battery array. It can be observed in Figure 6 that geometry 2 has less pressure drop in 58.86% than geometry 3 and 59.42% than geometry 1, being this the one that would require more pumping power, contrary to the maximum temperature of the system where geometry 1 turned out to have the lowest value, all this in terms of the base fluid. On the other hand, with respect to the nanofluids with a 0.5% concentration of nanoparticles, in terms of pressure drop, this increases with respect to the base fluid by 9.99% in geometry 2. After studying the case of the pressure difference with respect to other geometries, it can be seen that the pressure drop in the nanofluid with the concentration of 0.5% of nanoparticles is lower by 14.12% with respect to the concentration of 1.0% and 30.31% with respect to the concentration of 1.5%. Then, geometry 2 is the one that had a performance of interest in terms of pressure drop because its design is shorter in length than the other geometries. It is important to note that nanofluids are more viscous than the base fluid due to the internal forces of the nanoparticles in the fluid, so these cause a resistance to flow and therefore the pressure drop increases as the percentage of nanoparticles increases.

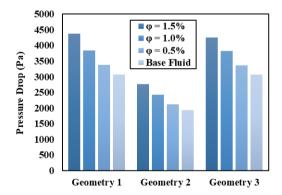


Figure 6. Pressure drop of the different geometries along the serpentine tube using water - ethylene glycol at 50% each and nanofluids (1.5%, 1.0%, 0.5% nanoparticles) as coolant

Figure 7 shows the effect of the different inlet velocities of the coolant flow on the average outlet temperature, observing that the higher the inlet velocity, the lower the temperature. In geometry 1 it is observed that at 0.1 m/s inlet velocity the average outlet temperature is 320.14 K, increasing this temperature by 6.28% and 14.13% at speeds of 0.09 m/s and 0.08 m/s respectively, this happens proportionally in the other geometries. A balance must be found for this speed since a high value as seen decreases the outlet temperature, but the system will need more coolant flow to compensate for the lower heat absorption per unit volume, while a low value of the speed reduces the efficiency of heat exchange between the coolant and the serpentine tube, this can cause overheating of the battery.

Finally in Figure 8, the effect of the different refrigerant

flow inlet velocities can also be seen but this time on the pressure drop, now geometry 2 is analyzed, due to its lower pressure drop value where the higher the inlet velocity, the pressure drop also increases, the latter may be inefficient because for higher speed a more powerful pump that will increase the energy consumption of the EV will be needed. It is observed that at 0.08 m/s the pressure is 2328.62 Pa, increasing by 18.81% and 38.26% for the 0.09 m/s and 0.08 m/s velocities. Having a very low pressure drop is also bad because it indicates a very low velocity which could cause overheating.

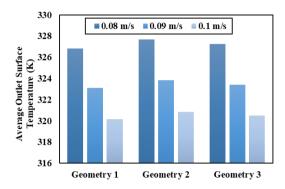


Figure 7. Average outlet temperature of different geometries at different speeds using 1.5% nanoparticle nanofluids as coolant

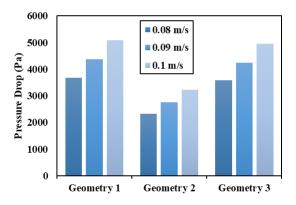


Figure 8. Pressure drop of different geometries at different velocities using 1.5% nanoparticle nanofluids as coolant

Already seen the results of the simulations it can be seen that the use of other geometries aimed at improving both the temperature that can serve for various applications other than EVs such as cooling in data center, high power electronics, turbines, reactors, HVAC (Heating, Ventilation and Air Conditioning) systems, among other applications, also with the improvement in the pressure drop helps the pump does not work so much and therefore less energy is spent to drive it, problems such as cavitation and overheating. All the damage that can be caused by excessive overheating, can lead to a decrease in service life, wear of various components or constant maintenance, that is why the use of nanofluids with precise geometries to mitigate these problems save energy and reduce economic expenditure.

4. CONCLUSIONS

In this research, a numerical study of the thermal and hydraulic performance of a serpentine tube used in the battery cooling system of an electric vehicle was performed using three different volume concentrations of aluminum oxide nanoparticles suspended in the working fluid used in these vehicles. Two additional arrangements of the serpentine tube were proposed in addition to the conventional arrangement used in commercial electric vehicles. As seen in the previous chapters, the following conclusions can be drawn:

- According to the temperature distribution, geometry 1, which is the conventional serpentine tube arrangement, is probably not the most suitable for this type of system. This is due to the fact that in the last section of the serpentine tube path the temperature rises, which could cause premature defects in the batteries according to their critical working temperature. In parallel, geometry 3, in spite of having a higher maximum working temperature, presented a more adequate temperature distribution for this type of system.
- According to the pressure drop, it was observed that geometry 1 and geometry 2 presented very similar values. However, in the case of geometry 2, a lower pressure drop value was obtained, and consequently a lower pumping power required, which leads to the conclusion that this geometry has a better hydraulic performance. With respect to the speed, this value should be moderate, because a high or very low speed can negatively affect the system.
- The change in the thermophysical properties of the nanofluids places them as potential fluids in thermal applications, however, it is advisable to evaluate the hydraulic performance of the systems to be used.

Future studies are expected to consider the use of more than one flow path instead of only one in the serpentine tube distributions in order to reduce the maximum temperature of the system in general. The analysis can also be performed with other arrays, adapting them to other types of batteries. And validate all these results experimentally on a test bench or an electric vehicle that represents a real environment.

REFERENCES

- [1] Cuéllar-Álvarez, Y., Clappier, A., Osses, M., Thunis, P., Belalcázar-Cerón, L.C. (2022). Well-to-wheel emissions and abatement strategies for passenger vehicles in two Latin American cities. Environmental Science and Pollution Research, 29(47): 72074-72085. https://doi.org/10.1007/s11356-022-20885-9
- [2] Zhang, W., Fang, X., Sun, C. (2023). The alternative path for fossil oil: Electric vehicles or hydrogen fuel cell vehicles. Journal of Environmental Management, 341: 118019. https://doi.org/10.1016/j.jenvman.2023.118019
- [3] Li, Z., Gao, M., Zhao, X., Cai, X., Zhang, Y. (2024). Heat generation effect and failure mechanism of pouch-type lithium-ion battery under over-discharge for electric vehicle. Journal of Energy Storage, 76: 109759. https://doi.org/10.1016/j.est.2023.109759
- [4] Yang, W., Zhou, F., Zhou, H., Wang, Q., Kong, J. (2020). Thermal performance of cylindrical lithium-ion battery thermal management system integrated with minichannel liquid cooling and air cooling. Applied Thermal Engineering, 175: 115331. https://doi.org/10.1016/j.applthermaleng.2020.115331
- [5] Sarchami, A., Tousi, M., Kiani, M., Arshadi, A., Najafi, M., Darab, M., Houshfar, E. (2022). A novel nanofluid

- cooling system for modular lithium-ion battery thermal management based on wavy/stair channels. International Journal of Thermal Sciences, 182: 107823. https://doi.org/10.1016/j.ijthermalsci.2022.107823
- [6] Saha, S.K., Ranjan, H., Emani, M.S., Bharti, A.K. (2020). Heat Transfer Enhancement in Externally Finned Tubes and Internally Finned Tubes and Annuli. SpringerBriefs in Applied Sciences and Technology. https://doi.org/10.1007/978-3-030-20748-9
- [7] Adhikari, N., Bhandari, R., Joshi, P. (2024). Thermal analysis of lithium-ion battery of electric vehicle using different cooling medium. Applied Energy, 360: 122781. https://doi.org/10.1016/j.apenergy.2024.122781
- [8] Tete, P.R., Gupta, M.M., Joshi, S.S. (2021). Developments in battery thermal management systems for electric vehicles: A technical review. Journal of Energy Storage, 35: 102255. https://doi.org/10.1016/j.est.2021.102255
- [9] Bhatti, M.M. (2021). Recent trends in nanofluids. Inventions, 6(2): 39. https://doi.org/10.3390/inventions6020039
- [10] Rashidi, S., Hormozi, F., Karimi, N., Ahmed, W. (2021). Applications of nanofluids in thermal energy transport. Emerging Nanotechnologies for Renewable Energy, pp. 345-368. https://doi.org/10.1016/b978-0-12-821346-9.00018-3
- [11] Singh, L.K., Mishra, G., Sharma, A.K., Gupta, A.K. (2021). A numerical study on thermal management of a lithium-ion battery module via forced-convective air cooling. International Journal of Refrigeration, 131: 218-234. https://doi.org/10.1016/j.ijrefrig.2021.07.031
- [12] Zhao, G., Wang, X., Negnevitsky, M., Zhang, H. (2021). A review of air-cooling battery thermal management systems for electric and hybrid electric vehicles. Journal of Power Sources, 501: 230001. https://doi.org/10.1016/j.jpowsour.2021.230001
- [13] Xiao, H., E, J., Tian, S., Huang, Y., Song, X. (2024). Effect of composite cooling strategy including phase change material and liquid cooling on the thermal safety performance of a lithium-ion battery pack under thermal runaway propagation. Energy, 295: 131093. https://doi.org/10.1016/j.energy.2024.131093
- [14] Zhang, Z., Wei, K. (2020). Experimental and numerical study of a passive thermal management system using flat heat pipes for lithium-ion batteries. Applied Thermal Engineering, 166: 114660. https://doi.org/10.1016/j.applthermaleng.2019.114660
- [15] Xu, J., Lan, C., Qiao, Y., Ma, Y. (2017). Prevent thermal runaway of lithium-ion batteries with minichannel cooling. Applied Thermal Engineering, 110: 883-890. https://doi.org/10.1016/j.applthermaleng.2016.08.151
- [16] Aldosry, A.M., Zulkifli, R., Wan Ghopa, W.A. (2021). Heat transfer enhancement of liquid cooled copper plate with oblique fins for electric vehicles battery thermal management. World Electric Vehicle Journal, 12(2): 55. https://doi.org/10.3390/wevj12020055
- [17] Chung, Y., Kim, M.S. (2019). Thermal analysis and pack level design of battery thermal management system with liquid cooling for electric vehicles. Energy Conversion and Management, 196: 105-116. https://doi.org/10.1016/j.enconman.2019.05.083
- [18] Saw, L.H., Ye, Y., Yew, M.C., Chong, W.T., Yew, M.K., Ng, T.C. (2017). Computational fluid dynamics simulation on open cell aluminium foams for Li-ion

- battery cooling system. Applied Energy, 204: 1489-1499. https://doi.org/10.1016/j.apenergy.2017.04.022
- [19] Pety, S.J., Tan, M.H.Y., Najafi, A.R., Barnett, P.R., Geubelle, P.H., White, S.R. (2017). Carbon fiber composites with 2D microvascular networks for battery cooling. International Journal of Heat and Mass Transfer, 115: 513-522. https://doi.org/10.1016/j.iiheatmasstransfer.2017.07.047
- [20] Al-Zareer, M., Dincer, I., Rosen, M.A. (2019). Development and analysis of a new tube based cylindrical battery cooling system with liquid to vapor phase change. International Journal of Refrigeration, 108: 163-173. https://doi.org/10.1016/j.ijrefrig.2019.08.027
- [21] Togun, H., Sultan Aljibori, H.S., Biswas, N., Mohammed, I.H., Sadeq, A.M., Lafta Rashid, F., Abdulrazzaq, T., Ali Zearah, S. (2024). A critical review on the efficient cooling strategy of batteries of electric vehicles: Advances, challenges, future perspectives. Renewable and Sustainable Energy Reviews, 203: 114732. https://doi.org/10.1016/j.rser.2024.114732
- [22] Lu, M., Zhang, X., Ji, J., Xu, X., Zhang, Y. (2020). Research progress on power battery cooling technology for electric vehicles. Journal of Energy Storage, 27: 101155. https://doi.org/10.1016/j.est.2019.101155
- [23] Thakur, A.K., Prabakaran, R., Elkadeem, M.R., Sharshir, S.W., Arıcı, M., Wang, C., Zhao, W., Hwang, J.Y., Saidur, R. (2020). A state of art review and future viewpoint on advance cooling techniques for Lithiumion battery system of electric vehicles. Journal of Energy Storage, 32: 101771. https://doi.org/10.1016/j.est.2020.101771
- [24] Xia, G., Cao, L., Bi, G. (2017). A review on battery thermal management in electric vehicle application. Journal of Power Sources, 367: 90-105. https://doi.org/10.1016/j.jpowsour.2017.09.046
- [25] Jarrett, A., Kim, I.Y. (2011). Design optimization of electric vehicle battery cooling plates for thermal performance. Journal of Power Sources, 196(23): 10359-10368. https://doi.org/10.1016/j.jpowsour.2011.06.090
- [26] Jarrett, A., Kim, I.Y. (2014). Influence of operating conditions on the optimum design of electric vehicle battery cooling plates. Journal of Power Sources, 245: 644-655.
 - https://doi.org/10.1016/j.jpowsour.2013.06.114
- [27] Kshetrimayum, K.S., Yoon, Y.G., Gye, H.R., Lee, C.J. (2019). Preventing heat propagation and thermal runaway in electric vehicle battery modules using integrated PCM and micro-channel plate cooling system. Applied Thermal Engineering, 159: 113797. https://doi.org/10.1016/j.applthermaleng.2019.113797
- [28] Benabdelaziz, K., Lebrouhi, B., Maftah, A., Maaroufi, M. (2020). Novel external cooling solution for electric vehicle battery pack. Energy Reports, 6: 262-272. https://doi.org/10.1016/j.egyr.2019.10.043
- [29] Ouyang, T., Liu, B., Wang, C., Ye, J., Liu, S. (2023). Novel hybrid thermal management system for preventing Li-ion battery thermal runaway using nanofluids cooling. International Journal of Heat and Mass Transfer, 201: 123652. https://doi.org/10.1016/j.ijheatmasstransfer.2022.12365
- [30] Sirikasemsuk, S., Wiriyasart, S., Prurapark, R., Naphon, N., Naphon, P. (2021). Water/nanofluid pulsating flow in thermoelectric module for cooling electric vehicle

- battery systems. International Journal of Heat and Technology, 39(5): 1618-1626. https://doi.org/10.18280/ijht.390525
- [31] Zhou, Z., Lv, Y., Qu, J., Sun, Q., Grachev, D. (2021). Performance evaluation of hybrid oscillating heat pipe with carbon nanotube nanofluids for electric vehicle battery cooling. Applied Thermal Engineering, 196: 117300.
 - https://doi.org/10.1016/j.applthermaleng.2021.117300
- [32] Sarchami, A., Kiani, M., Najafi, M., Houshfar, E. (2023). Experimental investigation of the innovated indirect-cooling system for Li-ion battery packs under fast charging and discharging. Journal of Energy Storage, 61: 106730. https://doi.org/10.1016/j.est.2023.106730
- [33] Czaplicka, N., Grzegórska, A., Wajs, J., Sobczak, J., Rogala, A. (2021). Promising nanoparticle-based heat transfer fluids-environmental and techno-economic analysis compared to conventional fluids. International Journal of Molecular Sciences, 22(17): 9201. https://doi.org/10.3390/ijms22179201
- [34] Canazas, J., Kamyshnikov, O. (2022). Heat transfer and pressure drop performance of a hydraulic mining shovel radiator by using ethylene glycol/water-based Al₂O₃ nanofluids. International Journal of Heat and Technology, 40(1): 273-281. https://doi.org/10.18280/ijht.400132
- [35] ASHRAE. (2017). ASHRAE Handbook: Fundamentals. American Society of Heating, Refrigerating and Air-Conditioning Engineers, Atlanta, GA.
- [36] Xuan, Y., Roetzel, W. (2000). Conceptions for heat transfer correlation of nanofluids. International Journal of Heat and Mass Transfer, 43(19): 3701-3707. https://doi.org/10.1016/s0017-9310(99)00369-5
- [37] Chiam, H.W., Azmi, W.H., Usri, N.A., Mamat, R., Adam, N.M. (2017). Thermal conductivity and viscosity of Al₂O₃ nanofluids for different based ratio of water and ethylene glycol mixture. Experimental Thermal and Fluid Science, 81: 420-429. https://doi.org/10.1016/j.expthermflusci.2016.09.013
- [38] Syam Sundar, L., Venkata Ramana, E., Singh, M.K., Sousa, A.C.M. (2014). Thermal conductivity and viscosity of stabilized ethylene glycol and water mixture Al₂O₃ nanofluids for heat transfer applications: An experimental study. International Communications in Heat and Mass Transfer, 56: 86-95. https://doi.org/10.1016/j.icheatmasstransfer.2014.06.00
- [39] Wiriyasart, S., Hommalee, C., Sirikasemsuk, S., Prurapark, R., Naphon, P. (2020). Thermal management system with nanofluids for electric vehicle battery cooling modules. Case Studies in Thermal Engineering, 18: 100583. https://doi.org/10.1016/j.csite.2020.100583
- [40] Saeed, A., Karimi, N., Paul, M.C. (2021). Analysis of the unsteady thermal response of a Li-ion battery pack to dynamic loads. Energy, 231: 120947. https://doi.org/10.1016/j.energy.2021.120947

NOMENCLATURE

- c specific heat, J. kg⁻¹. K⁻¹
- k thermal conductivity, W. m⁻¹. K⁻¹
- T temperature, K
- p pressure, Pa

u,v,w	velocity components along the x, y and z directions, respectively, m. s ⁻¹	ф	volume fraction, %
x,y,z	cartesian coordinates along the surface and normal to it, respectively	Subscripts	
Greek symbol	s	bf nf np	base fluid nanofluid nanoparticles
ρ μ	density, kg. m ⁻³ dynamic viscosity, Pa.s	-	-